

Sequential Markov Chain Monte Carlo for Filtering of State-Space Models with Low or Degenerate Observation Noise

BY ABYLAY ZHUMEKENOV¹, ALEXANDROS BESKOS², DAN CRISAN³, AJAY JASRA¹ & NIKOLAS KANTAS³

¹School of Data Science, The Chinese University of Hong Kong, Shenzhen, Shenzhen, CN.

²Department of Statistical Science, University College London, London, WC1E 6BT, UK

³Department of Mathematics, Imperial College London, London, SW7 2AZ, UK

E-Mail: abylayzhumekenov@cuhk.edu.cn; a.beskos@ucl.ac.uk; d.crisan@ic.ac.uk; ajayjasra@cuhk.edu.cn; n.kantas@ic.ac.uk

Abstract

We consider the discrete-time filtering problem in scenarios where the observation noise is degenerate or low. More precisely, one is given access to a discrete time observation sequence which at any time k depends only on the state of an unobserved Markov chain. We specifically assume that the functional relationship between observations and hidden Markov chain has either degenerate or low noise. In this article, under suitable assumptions, we derive the filtering density and its recursions for this class of problems on a specific sequence of manifolds defined through the observation function. We then design sequential Markov chain Monte Carlo methods to approximate the filter serially in time. For a certain linear observation model, we show that using sequential Markov chain Monte Carlo for low noise will converge as the noise disappears to that of using sequential Markov chain Monte Carlo for degenerate noise. We illustrate the performance of our methodology on several challenging stochastic models deriving from Statistics and Applied Mathematics.

Key words: Observation Noise, Filtering, Manifold Markov Chain Monte Carlo.

1 Introduction

We consider the following filtering problem (e.g. [2]). We have access to discrete-time observations $Y_1, Y_2, \dots, Y_k \in \mathbb{R}^{d_y}$, $k \in \mathbb{N}$, that are associated to an unobserved discrete-time Markov chain $X_0, X_1, \dots, X_k \in \mathbb{R}^{d_x}$, $k \in \mathbb{N}$. It is supposed that at any time $k \in \mathbb{N}$ we can write either

$$\begin{aligned} Y_k &= h_k(X_k), & \text{degenerate noise,} \\ Y_k &= \tilde{h}_k(X_k, \epsilon_k), & \text{low noise,} \end{aligned}$$

where $h_k : \mathbb{R}^{d_x} \rightarrow \mathbb{R}^{d_y}$ is not injective and $\epsilon_1, \epsilon_2, \dots$ is an independent and identically distributed (i.i.d.) sequence of \mathbb{R}^{d_y} random variables with ‘small variance’, $\tilde{h}_k : \mathbb{R}^{d_x} \times \mathbb{R}^{d_y} \rightarrow \mathbb{R}^{d_y}$. To substantiate the phrase small variance, one could imagine that ϵ_k has a d_y -dimensional Gaussian distribution of mean zero and covariance $\Delta \mathbf{I}_{d_y}$ with $\Delta > 0$ but close to zero and \mathbf{I}_{d_y} the $d_y \times d_y$ identity matrix. The objective of either the degenerate or low (or small) noise case, assuming it is well-defined, is to estimate expectations with respect to (w.r.t.) the conditional distribution of X_k given all the observations up-to time k , $Y_{1:k} = (y_1, \dots, y_k)^\top$, recursively in time. These problems are important in many applications in filtering problems where it is expected that the signal dynamics (unobserved Markov chain) is strongly driving the observed data; see for instance [3, 17, 30] for several applications.

Understanding filtering in the low noise regime has attracted long interest in the past from researchers focusing on continuous time dynamics and devising robust (extended) Kalman-Bucy type approximations of the filter [7, 20, 23, 26, 27] or establishing large deviations results for low Δ [16, 25], see also [21] for a recent review. In general, we need to stress that the filtering distributions are typically analytically intractable except in fairly simple models, such as ones involving linear and Gaussian dynamics. Using analytical approximations such as the extended Kalman filter or variants are biased and most often do not perform well for a many models. As a result, there is a vast literature in designing numerical algorithms based on Monte Carlo for approximating the filter; we refer the reader to [2, 11] and the references therein

for a complete treatment. In this article we focus upon developing Monte Carlo based algorithms for approximating the filter for degenerate or low noise case. Perhaps the most popular simulation method for low-dimensional filtering problems ($d_x \in \{1, 2, \dots, 10\}$) is the particle filter (PF) (see e.g. [2, 11]) which entails sampling $N \in \mathbb{N}$ particles in parallel, with the particles undergoing sampling, weighting and resampling operations. There are several related methods in high-dimensions such as [5, 28] and the approach that we are to focus upon is sequential Markov chain Monte Carlo (SMCMC) [4, 9, 22] which has been shown to be one of the most competitive methods (at least empirically) when trying to approximate the filter in high-dimensions [29].

The main issue that we deal with in this article is the appropriate formulation of the filter in a manner that takes into consideration the observation regime of interest and the corresponding development of effective computational approximations. In the degenerate noise case, we follow works such as [12, 14, 15] in defining the filter on a manifold $M_k = \{x \in \mathbb{R}^{d_x} : y_k - h_k(x) = 0\}$. In general, this manifold has zero Lebesgue measure and one must seek to derive a filter w.r.t. a more appropriate dominating measure. Under appropriate mathematical conditions we are able to derive the filtering density and the traditional filtering recursions of this density w.r.t. the Riemannian measure, i.e. we focus on the case where we can perform filtering on Riemannian manifolds. Previously, [18] also considered defining the filter along these lines, but focused only on continuous time dynamics for X and did not provide filtering recursions useful for discrete time models or appropriate numerical methods, which is the focus of this paper. We further show that the low-noise case can be cast in a similar framework and this can have substantial benefits in designing efficient numerical methods that are robust to very low observation noise. Having formulated the filter and its recursions we then seek to design computational methods for its approximation. Generic particle filtering or SMCMC methodologies referenced in the previous paragraph are not designed for filtering with degenerate noise. In particular, using a particle filter in the setting of interest in this work gives rise to some challenges:

1. In the context of degenerate noise one has to design importance sampling proposal dynamics that can move from one manifold to another.
2. In the small noise case, one expects that standard implementations of particle filters, oblivious to the prescribed model structure, will be rather inefficient, with a likely collapse of the importance weights to zero.

Whilst 1. is certainly an interesting open research question, it requires a substantial effort and then, at best, one can address low dimensional filtering problems. In 2. this circumvents the use of the PF in small noise filtering problems. In the context of using MCMC for sampling from probability measures defined on a manifold, there is already a substantial number of methods; a non-exhaustive list includes [6, 8, 14, 15, 31]. Given the success of the application of SMCMC in filtering in [29] it therefore seems natural to then design SMCMC for our class of filtering problems.

The main contributions of this article are as follows:

- Establishing a sequence of filtering densities w.r.t. the Riemannian measure, along with filtering recursions for the degenerate noise case and then extending this framework to encompass the low noise case.
- Designing SMCMC methods for the afore-mentioned filtering problems.
- In a particular scenario, proving that SMCMC in the small noise case will converge as the noise goes to zero, (marginally) to SMCMC in the degenerate noise problem.
- Implementing our methodology on several interesting models.

We note that given that we can design efficient methods for filtering in the degenerate noise case, by casting the low noise problem into a similar framework, with little extra effort we can carry out filtering for an arbitrarily low noise. In fact this approach will be robust to low levels of Δ and the convergence result mentioned in the third bullet means that this is an appropriate strategy when sampling for the limiting

degenerate case performs well. We stress that standard algorithms do not satisfy such a robustness criterion w.r.t. diminishing noise. This extends the appeal of the mathematical and computational approach in this article. Finally it is worth mentioning that there are different problems that X_k is naturally defined on manifold and this requires one to establish appropriate filtering equations, e.g. [10, 33] consider this in continuous-time. Here our setting is different and we establish filtering recursions on a sequence of manifolds (M_k) due to the constraint posed by the observations.

This article is structured as follows. In Section 2 we define the filtering problem of interest, which features our first mathematical result on defining the sequence of filtering probability measures. In Section 3 we present our sequential MCMC method. This section also gives the second mathematical result on proving that SMCMC in the small noise case will converge to SMCMC in the degenerate noise problem. In Section 4 we detail our numerical implementations. The proofs of our mathematical results can be found in Appendix A.

2 Filtering Problem

2.1 Model

We denote the measurable space of the d_x -dimensional real line with associated Borel σ -field $(\mathbb{R}^{d_x}, \mathcal{B}(\mathbb{R}^{d_x}))$ and set λ_{d_x} as the d_x -dimensional Lebesgue measure. We are given a discrete-time Markov Chain $\{X_k\}_{k \geq 0}$, $X_k \in \mathbb{R}^{d_x}$, with $X_0 = x_0 \in \mathbb{R}^{d_x}$ given and positive Lebesgue transition density $f_k : \mathbb{R}^{d_x} \times \mathbb{R}^{d_x} \rightarrow \mathbb{R}^+$, $k \in \mathbb{N}$. That is, for any $(k, x_{k-1}) \in \mathbb{N} \times \mathbb{R}^{d_x}$:

$$\int_{\mathbb{R}^{d_x}} f_k(x_{k-1}, x_k) \lambda_{d_x}(dx_k) = 1$$

and any $(k, A) \in \mathbb{N} \times \mathcal{B}(\mathbb{R}^{d_x})$

$$\int_A f_k(x_{k-1}, x_k) \lambda_{d_x}(dx_k)$$

is a measurable function. For any fixed $n \in \mathbb{N}$, the joint density, of the Markov chain w.r.t. $\bigotimes_{k=1}^n \lambda_{d_x}(dx_k)$ is

$$p_n(x_{1:n}) = \prod_{k=1}^n f_k(x_{k-1}, x_k).$$

We consider a sequence of observations $\{Y_k\}_{k \geq 1}$, $Y_k \in \mathbb{R}^{d_y}$ which are assumed such that for $h_k : \mathbb{R}^{d_x} \rightarrow \mathbb{R}^{d_y}$, $k \in \mathbb{N}$, we have

$$Y_k = h_k(X_k)$$

where h_k is not injective. The objective, assuming it is well-defined, is to approximate expectations of functions of X_k given all the observations $y_{1:k}$ at each time $k \in \mathbb{N}$ (i.e. filtering). We refer to this problem as ‘filtering with degenerate noise’. Throughout we will only be able to deal with models for which $d_x > d_y$ as we will define our filter on a $d_x - d_y$ submanifold of \mathbb{R}^{d_x} , with \mathbb{R}^{d_x} itself being the ambient space.

We will also consider the case that

$$Y_k = \tilde{h}_k(X_k, \epsilon_k) \tag{2.1}$$

where $\tilde{h}_k : \mathbb{R}^{d_x} \times \mathbb{R}^{d_y} \rightarrow \mathbb{R}^{d_y}$ where $\{\epsilon_k\}_{k \geq 0}$ is an independent and identically distributed (i.i.d.) sequence of noises which have zero mean and small variance; filtering in this context will be termed ‘filtering with low noise’. As we will see, this latter problem can be dealt with via an approach similar to the one developed for the degenerate case.

2.2 Filtering with Degenerate Noise

For each $k \in \mathbb{N}$ we write

$$c_k(x_k) = y_k - h_k(x_k).$$

For any fixed $n \in \mathbb{N}$ write $\mathbf{c}_n(x_{1:n}) := (c_1(x_1), \dots, c_n(x_n))^\top$. Introduce the manifold $\mathbf{M}_k = \{x \in \mathbb{R}^{d_x} : c_k(x) = 0\}$ and set $\mathbf{M}_n = \{x_{1:n} \in \mathbb{R}^{nd_x} : \mathbf{c}_k(x_{1:n}) = 0\} = \mathbf{M}_1 \times \dots \times \mathbf{M}_n$. Let $\{M_k\}_{k \geq 1}$ be any sequence of positive definite $d_x \times d_x$ matrices and we suppose that for each $k \in \mathbb{N}$, \mathbb{R}^{d_x} is equipped with a metric tensor with a fixed positive definite matrix representation M_k . For $n \in \mathbb{N}$ set $\mathbf{M}_n = \text{diag}(M_1, \dots, M_n)$ be a $nd_x \times nd_x$ block diagonal matrix. We suppose that for each $n \in \mathbb{N}$, \mathbb{R}^{nd_x} is equipped with a metric tensor with a fixed positive definite matrix representation \mathbf{M}_n . We will make the following assumption.

(A1) For each $k \in \mathbb{N}$, c_k is continuously differentiable and that the Jacobian ∂c_k has full row-rank.

For $k \in \mathbb{N}$, we denote by $\sigma_{\mathbf{M}_k}^{M_k}(dx_k)$ the Riemannian measure on the manifold \mathbf{M}_k ; see for instance [15, Lemma C.2.]. In effect, $\sigma_{\mathbf{M}_k}^{M_k}(dx_k)$ is the natural extension of a Lebesgue measure on a manifold, in the sense that, e.g., it can be used to measure surfaces on the manifold. For simplicity we write for $k \in \mathbb{N}$

$$g_k(x_k) = \det(\partial c_k(x_k) M_k^{-1} \partial c_k(x_k)^\top)^{-1/2}. \quad (2.2)$$

We will denote by π_k the filtering density, w.r.t. $\sigma_{\mathbf{M}_k}^{M_k}$ at any time $k \in \mathbb{N}$. We write the density as $\pi_k(x_k)$, that is, omitting making reference to the data in the notation. Our objective is estimate expectations w.r.t. the filter, that is for $\varphi : \mathbb{R}^{d_x} \rightarrow \mathbb{R}$ to estimate

$$\pi_k(\varphi) = \mathbb{E}[\varphi(X_k) | Y_{0:k}] = \int_{\mathbf{M}_k} \varphi(x_k) \pi_k(x_k) \sigma_{\mathbf{M}_k}^{M_k}(dx_k)$$

when φ is integrable w.r.t. $\pi_k(x_k) \sigma_{\mathbf{M}_k}^{M_k}(dx_k)$. In the following result we give a representation of the density π_k . The proof can be found in Appendix A.1.

Proposition 2.1. *Assume (A1). Then we have that*

$$\pi_1(x_1) = \frac{g_1(x_1) f_1(x_0, x_1)}{\int_{\mathbf{M}_1} g_1(x_1) f_1(x_0, x_1) \sigma_{\mathbf{M}_1}^{M_1}(dx_1)}$$

and for any $k \geq 2$ we have that

$$\pi_k(x_k) = \frac{g_k(x_k) \int_{\mathbf{M}_{k-1}} f_k(x_{k-1}, x_k) \pi_{k-1}(x_{k-1}) \sigma_{\mathbf{M}_{k-1}}^{M_{k-1}}(dx_{k-1})}{\int_{\mathbf{M}_k} g_k(x_k) \int_{\mathbf{M}_{k-1}} f_k(x_{k-1}, x_k) \pi_{k-1}(x_{k-1}) \sigma_{\mathbf{M}_{k-1}}^{M_{k-1}}(dx_{k-1}) \sigma_{\mathbf{M}_k}^{M_k}(dx_k)}. \quad (2.3)$$

Functions g_1, g_2, \dots are as defined in (2.2).

The significance of Proposition 2.1 is to demonstrate that under fairly general conditions one has a prediction-updating representation of the filtering density w.r.t. the Riemannian measure, in the case of degenerate noise. This formula is not surprising, given the previous work in e.g. [12, 15], but the formal statement is important in the computational methodology that we are to present. In essence we seek to construct a computational approach which can approximate this prediction-updating formula (2.3).

We note that the formulation of [15] considers the setting where $X_k = F_k(X_{k-1}, \nu_k)$ for $\{\nu_k\}_{k \geq 0}$ a sequence of i.i.d. noises with positive Lebesgue density and $F_k : \mathbb{R}^{2d_x} \rightarrow \mathbb{R}^{d_x}$. Under appropriate assumptions this allows one to define a type of filter on the *path-space* of noises $\nu_{1:k}$ at any time k . The details can be found in [15], but for the purpose of this discussion suppose given x_0 one has that $X_1 = F_1(x_0, \nu_1)$ and then for any subsequent $k \geq 2$, $X_k = F_k(F_{k-1} \circ \dots \circ F_1(x_0, \nu_1), \nu_k)$, which then induces a constraint $\mathbf{c}_k(\nu_{1:k}) = 0$. The motivation from [15] is that at each k this so-called collapsed representation (as per [24]) of the smoother/filter can facilitate MCMC algorithms targeting $\nu_{0:k}$, which can mix quickly, rather than working directly with the X_k 's. In the context of filtering, this approach can have two deficiencies:

1. The state-space of the filter grows with time.

2. The number of constraints grows with time.

Point 1. is well understood in the literature (e.g. [19]) and often leads to computational algorithms whose cost scales quadratically with the time parameter. In online problems (i.e. filtering) one often wants the computational cost to be fixed each time an observation is acquired so that long data sequences can be processed. On point 2. the issue is that when considering simulation methods to update all the $\nu_{1:k}$ one has to satisfy all of the constraints $\mathbf{c}_k(\nu_{1:k})$ simultaneously, which is possible, e.g. with MCMC [8, 14, 15, 31], but, unquestionably would add extra computational complexity to a simulation method. As a result, we have decided to work directly with the X_k 's as in Proposition 2.1.

2.3 Filtering with Low Noise

We now consider the case (2.1). Filtering with low noise of course, under appropriate assumptions, can be dealt with via a density w.r.t. d_x -dimensional Lebesgue measure. However, in a manner similar to the approach in [15] one can also consider an equivalent representation w.r.t. the Riemannian measure. We will explain the possible benefits from opting for such an approach when the noise has small variance below.

We give a formal presentation as above; the details are repeated for completeness. For each $k \in \mathbb{N}$ we write

$$\tilde{c}_k(x_k, \epsilon_k) = y_k - \tilde{h}_k(x_k, \epsilon_k).$$

For any fixed $n \in \mathbb{N}$ write $\tilde{\mathbf{c}}_n(x_{1:n}, \epsilon_{1:n}) := (\tilde{c}_1(x_1, \epsilon_1), \dots, \tilde{c}_n(x_n, \epsilon_n))^\top$. Set $\tilde{\mathbf{M}}_k = \{(x, \epsilon) \in \mathbb{R}^{d_x+d_y} : \tilde{c}_k(x, \epsilon) = 0\}$ and $\tilde{\mathbf{M}}_n = \{(x_{1:n}, \epsilon_{1:n}) \in \mathbb{R}^{n(d_x+d_y)} : \tilde{\mathbf{c}}_n(x_{1:n}, \epsilon_{1:n}) := 0\} = \tilde{\mathbf{M}}_1 \times \dots \times \tilde{\mathbf{M}}_n$. Let $\{\tilde{M}_k\}_{k \geq 1}$ be any sequence of positive definite $(d_x + d_y) \times (d_x + d_y)$ matrices and we suppose that for each $k \in \mathbb{N}$, \mathbb{R}^{2d_x} is equipped with a metric tensor with a fixed positive definite matrix representation \tilde{M}_k . For $n \in \mathbb{N}$ set $\tilde{\mathbf{M}}_n = \text{diag}(\tilde{M}_1, \dots, \tilde{M}_n)$ be the $n(d_x + d_y) \times n(d_x + d_y)$ block diagonal matrix. We suppose that for each $n \in \mathbb{N}$, $\mathbb{R}^{n(d_x+d_y)}$ is equipped with a metric tensor with a fixed positive definite matrix representation $\tilde{\mathbf{M}}_n$. We assume that: $p_{\mathbb{N}}$ is the positive Lebesgue density of the distribution of ϵ_1 ; for each $k \in \mathbb{N}$, \tilde{c}_k is continuously differentiable and that the Jacobian $\partial \tilde{c}_k$ has full row-rank. Then one can prove in a similar manner to Proposition 2.1 that the filtering density at time 1 w.r.t. $\sigma_{\tilde{\mathbf{M}}_1}^{\tilde{M}_1}$ is

$$\tilde{\pi}_1(x_1, \epsilon_1) = \frac{\tilde{g}_1(x_1, \epsilon_1) f_1(x_0, x_1) p_{\mathbb{N}}(\epsilon_1)}{\int_{\tilde{\mathbf{M}}_1} \tilde{g}_1(x_1, \epsilon_1) f_1(x_0, x_1) p_{\mathbb{N}}(\epsilon_1) \sigma_{\tilde{\mathbf{M}}_1}^{\tilde{M}_1}(d(x_1, \epsilon_1))}$$

and for any $k \geq 2$ we have that

$$\tilde{\pi}_k(x_k, \epsilon_k) = \frac{\tilde{g}_k(x_k, \epsilon_k) p_{\mathbb{N}}(\epsilon_k) \int_{\tilde{\mathbf{M}}_{k-1}} f_k(x_{k-1}, x_k) \tilde{\pi}_{k-1}(x_{k-1}, \epsilon_{k-1}) \sigma_{\tilde{\mathbf{M}}_{k-1}}^{\tilde{M}_{k-1}}(d(x_{k-1}, \epsilon_{k-1}))}{\int_{\tilde{\mathbf{M}}_k} \tilde{g}_k(x_k, \epsilon_k) p_{\mathbb{N}}(\epsilon_k) \int_{\tilde{\mathbf{M}}_{k-1}} f_k(x_{k-1}, x_k) \tilde{\pi}_{k-1}(x_{k-1}, \epsilon_{k-1}) \sigma_{\tilde{\mathbf{M}}_{k-1}}^{\tilde{M}_{k-1}}(d(x_{k-1}, \epsilon_{k-1})) \sigma_{\tilde{\mathbf{M}}_k}^{\tilde{M}_k}(d(x_k, \epsilon_k))}$$

where

$$\tilde{g}_k(x_k, \epsilon_k) = \det \left(\partial \tilde{c}_k(x_k, \epsilon_k) \tilde{M}_k^{-1} \partial \tilde{c}_k(x_k, \epsilon_k)^\top \right)^{-1/2}.$$

The reason for this presentation is as follows. If one has a computational method that can efficiently approximate the filter in the degenerate noise case (i.e. π_k), then there is little complication to efficiently approximate the filter in the low noise case (i.e. $\tilde{\pi}_k$) and moreover there may be some type of convergence as the noise in the latter case disappears. More concretely, suppose that $\epsilon_k \stackrel{\text{i.i.d.}}{\sim} \mathcal{N}_{d_y}(0, \Delta \mathbf{I}_{d_y})$, where $\Delta > 0$ and $\mathcal{N}_{d_y}(0, \Delta \mathbf{I}_{d_y})$ is the d_y -dimensional Gaussian distribution of mean 0 and covariance Δ multiplied by the identity matrix \mathbf{I}_{d_y} . Then we might expect that if there is a computational method approximating $\{\tilde{\pi}_k\}_{k \geq 0}$ then as $\Delta \downarrow 0$ there is a mathematical convergence of this method (the notion of convergence is left deliberately vague, but is explored in Section 3.4) to some type of equivalent in the degenerate noise case. We note that popular sampling methods could fail to perform well in the low noise case. For

instance, one might expect quite sophisticated MCMC methods, such as [1], to have very poor mixing. Finally, the presentation for the low noise case includes also intermediate cases where $\tilde{h}_k(X_k, \epsilon_k)$ results to some coordinates of Y_k being deterministic and others containing some level of noise.

3 Methodology

In the following section we outline our methodology. All of the approaches are detailed in the degenerate noise case, but there is little modification needed for the low noise case. At the end, Section 3.4, we give our result on the convergence of SMCMC in the low noise case, to that in the degenerate case.

3.1 Basic Method

Our approach is to use sequential MCMC (SMCMC) which proceeds as follows. At time 1, one needs access to any ergodic Markov kernel $K_1 : \mathbb{R}^{d_x} \times \mathcal{B}(\mathbb{R}^{d_x}) \rightarrow [0, 1]$ that admits $\pi_1(x_1)\sigma_{M_1}^{M_1}(dx_1)$ as its invariant measure. Several candidates are available such as in [8, 14, 15, 31] and for completeness we detail the approach of [31] in Section 3.3.

The MCMC kernel will produce N samples which we denote $(x_1^1, \dots, x_1^N) \in M_1^N$. Now, the filter at time 2 as given in Proposition 2.1 is

$$\pi_2(x_2) = \frac{g_2(x_2) \int_{M_1} f_2(x_1, x_2) \pi_1(x_1) \sigma_{M_1}^{M_1}(dx_1)}{\int_{M_2} g_2(x_2) \int_{M_1} f_2(x_1, x_2) \pi_1(x_1) \sigma_{M_1}^{M_1}(dx_1) \sigma_{M_2}^{M_2}(dx_2)}$$

which for any given x_2 is not available to compute point-wise up-to a normalizing constant; this is a pre-requisite of using MCMC, which is our intention. The idea in SMCMC is to use the samples at the previous observation time, to approximate the density of the target at the current observation time. In this scenario, one would have the approximated density

$$\pi_2^N(x_2) \propto g_2(x_2) \frac{1}{N} \sum_{i=1}^N f_2(x_1^i, x_2)$$

w.r.t. $\sigma_{M_2}^{M_2}$. At this stage one may be tempted to sample from π_2^N , but this can be prohibitive from a computational cost perspective as the cost of computing π_2^N is $\mathcal{O}(N)$. Since one typically must compute π_2^N to simulate from an MCMC kernel of invariant measure $\pi_2^N(x_2)\sigma_{M_2}^{M_2}(dx_2)$, the cost to produce N samples is $\mathcal{O}(N^2)$ which can be too much for the approach to be practically useful.

We consider the following simple alternative. Let $s \in \{1, \dots, N\}$ be given and typically we want s to be much less than N . Define $\mathbb{I}_s = \{i_{1:s} \in \{1, \dots, N\}^s : i_1 \neq i_2 \neq \dots \neq i_s\}$ (write the power set of \mathbb{I}_s as \mathcal{I}_s), we then define the probability density

$$\widehat{\pi}_2^N(x_2, i_{1:s}) \propto g_2(x_2) \sum_{j \in \mathbb{I}_s} f_2(x_1^j, x_2)$$

w.r.t. $\sigma_{M_2}^{M_2} \otimes \mu_{\mathbb{I}_s}$, where $\mu_{\mathbb{I}_s}$ is the counting measure on \mathbb{I}_s . We note that it is straightforward to verify that:

$$\pi_2^N(x_2) = \sum_{i_{1:s} \in \mathbb{I}_s} \widehat{\pi}_2^N(x_2, i_{1:s})$$

so that one can sample directly from $\widehat{\pi}_2^N$ and the cost of computation is likely to be lower than dealing directly with $\pi_2^N(x_2)$. Then at time 2 one uses an MCMC kernel $K_2 : \mathbb{R}^{d_x} \times \mathbb{I}_s \times \mathcal{B}(\mathbb{R}^{d_x}) \times \mathcal{I}_s \rightarrow [0, 1]$ that admits $\widehat{\pi}_2^N(x_2, i_{1:s})\sigma_{M_2}^{M_2}(dx_2)\mu_{\mathbb{I}_s}(di_{1:s})$ as its invariant measure. The way in which this latter kernel is constructed is via a Metropolis-within-Gibbs method as we now detail. For any $i_{1:s} \in \mathbb{I}_s$ given, let $\widehat{K}_2 : \mathbb{R}^{d_x} \times \mathbb{I}_s \times \mathcal{B}(\mathbb{R}^{d_x}) \rightarrow [0, 1]$ be an ergodic Markov-kernel of invariant measure proportional to

$\widehat{\pi}_2^N(x_2, i_{1:s})\sigma_{M_2}^{M_2}(dx_2)$ (such as in [8, 14, 15, 31]). Then \widehat{K}_2 is used to sample from the full-conditional of X_2 given $i_{1:s}$. Let $x_2 \in M_2$ be given and let $\check{K}_2 : \mathbb{R}^{d_x} \times I_s \times \mathcal{I}_s \rightarrow [0, 1]$ be an ergodic Markov kernel of invariant measure proportional to $\widehat{\pi}_2^N(x_2, i_{1:s})\mu_{I_s}(di_{1:s})$; a simple example is a Metropolis-Hastings kernel. Then we set

$$K_2((x_2, i_{1:s}), (dx'_2, di'_{1:s})) = \widehat{K}_2((x_2, i_{1:s}), dx'_2) \check{K}_2((x'_2, i_{1:s}), di'_{1:s}).$$

One can produce N samples $(x_2^1, \dots, x_2^N) \in M_2^N$ and so one can repeat this idea again at time step 3 and later times.

3.2 Final Algorithm

Our final method will be as follows. One must choose $(N, s) \in \mathbb{N} \times \{1, \dots, N\}$ from the beginning.

1. Initialization. Run an ergodic Markov kernel $K_1 : \mathbb{R}^{d_x} \times \mathcal{B}(\mathbb{R}^{d_x}) \rightarrow [0, 1]$ that admits $\pi_1(x_1)\sigma_{M_1}^{M_1}(dx_1)$ as its invariant measure for N steps, giving $(X_1^1, \dots, X_1^N) \in M_1^N$. The initial sample $X_1^0 \in M_1$ can be obtained, for example, using a deterministic root-finding method. Set $k = 2$ and go to Step 2..
2. Observation iteration at time $k \geq 2$. We are given $(x_{k-1}^1, \dots, x_{k-1}^N) \in M_{k-1}^N$ from the previous time step. Let $K_k : \mathbb{R}^{d_x} \times I_s \times \mathcal{B}(\mathbb{R}^{d_x}) \vee \mathcal{I}_s \rightarrow [0, 1]$ be an ergodic Markov kernel with invariant measure $\widehat{\pi}_k^N(x_k, i_{1:s})\sigma_{M_k}^{M_k}(dx_k)\mu_{I_s}(di_{1:s})$ where

$$\widehat{\pi}_k^N(x_k, i_{1:s}) \propto g_k(x_k) \sum_{j \in I_s} f_k(x_1^j, x_k).$$

Run K_k for N steps, giving $(X_k^1, \dots, X_k^N) \in M_k^N$. The initial sample $X_k^0 \in M_k$ can be obtained, for example, using a deterministic root-finding method. Set $k = k + 1$ and go to the start of Step 2..

Recall that we will set

$$K_k((x_k, i_{1:s}), (dx'_k, di'_{1:s})) = \widehat{K}_k((x_k, i_{1:s}), dx'_k) \check{K}_k((x'_k, i_{1:s}), di'_{1:s})$$

where \widehat{K}_k has, for $i_{1:s} \in I_s$ fixed, invariant measure proportional to $\widehat{\pi}_k^N(x_k, i_{1:s})\sigma_{M_k}^{M_k}(dx_k)$ and for $x_k \in M_k$ fixed, \check{K}_k is (for instance) a Metropolis-Hastings kernel that has invariant measure proportional to $\widehat{\pi}_k^N(x_k, i_{1:s})\mu_{I_s}(di_{1:s})$. We note that the computational cost of the method is approximately the same at every observation time making it a truly online method. As noted in the introduction, it circumvents having to design proposals moving from one manifold to the next, which would seem to be a requirement of traditional particle filtering approaches.

The SMC-MCMC method allows one to approximate $\pi_k(\varphi)$ for any $k \in \mathbb{N}$ using

$$\pi_k^N(\varphi) = \frac{1}{N} \sum_{i=1}^N \varphi(x_k^i).$$

Under appropriate assumptions, it is possible to show convergence of this estimator (in an almost sure sense) to $\pi_k(\varphi)$ as $N \rightarrow \infty$; see [22]. An important remark is that if manifold MCMC methods are too expensive, one could relax the problem and consider approximate manifold MCMC as in [13].

3.3 Example of a MCMC Kernel for manifolds

In order to demonstrate that MCMC methods on manifolds are possible, we quickly review the method of [31] as it will be used in Section 4. We do not include complete details and these can be found in [31].

For simplicity of exposition we shall consider sampling for $k = 1$ from $\pi_1(x_1)\sigma_{M_1}^{M_1}(dx_1)$, but a modification to other contexts is fairly simple to derive. Let $x \in M_1$ and denote the tangent space of x as T_x and T_x^\perp as the orthogonal space. We begin at a point $x \in M_1$ and we now show how the next point in the Markov chain is generated.

- Compute the Q-R decomposition of $\partial c_1(x)^\top$. Denote by U_x the $(d_x - d_y) \times d_x$ matrix that is obtained from the last $d_x - d_y$ columns of the Q-R decomposition just computed.
- Sample $Z \sim \mathcal{N}_{d_x - d_y}(0, \mathbb{I}_{d_x - d_y})$. Set $v = \rho U_x^\top Z \in \mathbb{R}^x$, where $\rho > 0$ is a user-specified constant.
- Find $a \in \mathbb{R}^{d_y}$ such that

$$c_1(x + v + w) = 0$$

where $\partial c_1(x)_i$ is the i^{th} row of $\partial c_1(x)$ and $w = \sum_{i=1}^{d_y} a_i (\partial c_1(x)_i)^\top$. Set $y = x + v + w \in \mathbb{M}_1$.

- Determine $(v', w') \in \mathbb{T}_y \times \mathbb{T}_y^\perp$, where $x - y = v' + w'$. This is possible by projecting $x - y$ onto \mathbb{T}_y and \mathbb{T}_y^\perp via the Q-R decomposition of $\partial c_1(y)^\top$, i.e. via U_y the $(d_x - d_y) \times d_x$ matrix that is obtained from the last $d_x - d_y$ columns of the Q-R decomposition of $\partial c_1(y)^\top$.
- Generate $R \sim \mathcal{U}_{[0,1]}$ (uniform distribution on $[0, 1]$) and accept y as the new state of the Markov chain if:

$$R < \min \left\{ 1, \frac{\pi_1(y)q(v'|x)}{\pi_1(x)q(v|x)} \right\}$$

where $q(v|x)$ is the density of a $\mathcal{N}_{d_x}(0, \rho^2 U_x^\top U_x)$ random variable evaluated at v and $q(v'|y)$ is the density of a $\mathcal{N}_{d_x}(0, \rho^2 U_y^\top U_y)$ random variable evaluated at v' . Otherwise stay at x .

There is an important point which is omitted in the above steps. If in bullet 3 one has a pre-specified root finding method (e.g. Newton) with some pre-specified parameters (for example a maximum number of iterations) then one must check in bullet point 4 if x can be obtained from y, v' using the same root finding method. If it cannot be, then the move is immediately rejected. Work [31] provides a complete explanation.

3.4 Convergence of Low Noise to Degenerate Noise Case

In this section we consider a special case of the filtering problem and the convergence, in an appropriate sense, of the low noise sequential MCMC method; we now give the details. We restrict ourselves to the model that for each $k \in \mathbb{N}$:

$$Y_k = A_k X_k + \Delta^{1/2} \epsilon_k$$

where $\{A_k\}_{k \geq 1}$ is a sequence of $d_y \times d_x$ real matrices with full row rank, $d_x > d_y$, $\epsilon_k \stackrel{\text{i.i.d.}}{\sim} \mathcal{N}_{d_y}(0, \mathbb{I}_{d_y})$ and $\Delta > 0$ for the low noise filter, whereas $\Delta = 0$ for the corresponding degenerate noise filter. For the dynamics $\{X_k\}_{k \geq 0}$ we do not make any assumptions except that the Lebesgue transition density $f_k(x_{k-1}, x_k)$ can be evaluated pointwise. In the sequel we will sometimes refer to the low noise filter and other times to the degenerate noise one. The distinction will be obvious from the context and the particular notation used in each setting.

As the sequence of manifolds $\tilde{\mathbb{M}}_k$ (resp. \mathbb{M}_k) are determined via linear constraints, it is possible in this setting to specify Lebesgue densities of the filters on d_x -dimensional (resp. $(d_x - d_y)$ -dimensional) spaces. At time k we use $\tilde{Z}_k \in \mathbb{R}^{d_x}$ to denote the unknown random variable associated to the filter at time k of the low noise problem, and use the notation $\tilde{Z}_k = (Z_k, \bar{Z}_k)^\top$ where $Z_k \in \mathbb{R}^{d_x - d_y}$ and $\bar{Z}_k \in \mathbb{R}^{d_y}$. We can write the Lebesgue density $\tilde{\pi}_k^\lambda(\tilde{z}_k)$ in the following manner. Let $A_k^\Delta := [A_k, \Delta^{1/2} \mathbb{I}_{d_y}]$ be a $d_y \times (d_x + d_y)$ matrix, define $\ker(A_k^\Delta) := \{x \in \mathbb{R}^{d_x + d_y} : A_k^\Delta x = 0\}$, let V_k^Δ be a $(d_x + d_y) \times d_x$ matrix whose columns are an orthonormal basis of $\ker(A_k^\Delta)$ and \tilde{z}_k^Δ be a $(d_x + d_y)$ -dimensional vector that solves $Y_k = A_k^\Delta \tilde{z}_k^\Delta$. To compute \tilde{z}_k^Δ , let z_k^* be any d_x -dimensional vector that solves $Y_k = A_k z_k^*$, then we set $\tilde{z}_k^\Delta = (z_k^*, 0)^\top$. Finally for any $z \in \mathbb{R}^{d_x}$ set

$$u_k^\Delta(z) = \tilde{z}_k^\Delta + V_k^\Delta z$$

and we will use the convention that $u_k^\Delta(z) = (u_k^\Delta(z, x), u_k^\Delta(z, \epsilon))^\top$. $u_k^\Delta(z, x) \in \mathbb{R}^{d_x}$, $u_k^\Delta(z, \epsilon) \in \mathbb{R}^{d_y}$. Note also that $Y_k = A_k^\Delta u_k^\Delta(z)$. Then we have that

$$\tilde{\pi}_1^\lambda(\tilde{z}_1) \propto p_{\mathbb{N}}(u_1^\Delta(\tilde{z}_1, \epsilon)) f_1(x_0, u_1^\Delta(\tilde{z}_1, x))$$

and for any $k \geq 2$

$$\tilde{\pi}_k^\lambda(\tilde{z}_k) \propto p_N(u_k^\Delta(\tilde{z}_k, \epsilon)) \int_{\mathbb{R}^{d_x}} f_k(u_{k-1}^\Delta(\tilde{z}_{k-1}, x), u_k^\Delta(\tilde{z}_k, x)) \tilde{\pi}_{k-1}^\lambda(\tilde{z}_{k-1}) \lambda_{d_x}(d\tilde{z}_{k-1}).$$

For the case of the degenerate noise, we can write the Lebesgue density $\pi_k^\lambda(z_k)$ in a similar manner, which is added for completeness. Let $\ker(A_k) = \{x \in \mathbb{R}^{d_x} : A_k x = 0\}$, V_k^* be a $d_x \times (d_x - d_y)$ matrix whose columns are an orthonormal basis of $\ker(A_k)$ and z_k^* is as used above. For any $z \in \mathbb{R}^{d_x - d_y}$ set

$$u_k^*(z) = z_k^* + V_k^* z$$

and we note that $Y_k = A_k u_k^*(z)$. Then we have that

$$\pi_1^\lambda(z_1) \propto f_1(x_0, u_1^*(z_1))$$

and for any $k \geq 2$

$$\pi_k^\lambda(z_k) \propto \int_{\mathbb{R}^{d_x}} f_k(u_{k-1}^*(z_{k-1}), u_k^*(z_k)) \pi_{k-1}^\lambda(z_{k-1}) \lambda_{d_x - d_y}(dz_{k-1}).$$

For the MCMC kernels required by the SMCMC method, we will use in the low-noise case a sequence of random walk Metropolis kernels with Gaussian proposals in dimension d_x . We focus on the $\mathcal{O}(N^2)$ implementation (with $s = N$) for simplicity although relaxing this is a matter of changing the notations, rather than mathematical complexity. The MCMC kernel, $K_k^\Delta : \mathbb{R}^{d_x} \times \mathcal{B}(\mathbb{R}^{d_x}) \rightarrow [0, 1]$, can be described at any time $k \geq 2$, for $(\tilde{z}_{k-1}^1, \dots, \tilde{z}_{k-1}^N) \in \mathbb{R}^{Nd_x}$ given

$$\begin{aligned} K_k^\Delta(\tilde{z}, d\tilde{z}') &= \min \left\{ 1, \frac{p_N(u_k^\Delta(\tilde{z}', \epsilon)) \frac{1}{N} \sum_{i=1}^N f_k(u_{k-1}^\Delta(\tilde{z}_{k-1}^i, x), u_k^\Delta(\tilde{z}', x))}{p_N(u_k^\Delta(\tilde{z}, \epsilon)) \frac{1}{N} \sum_{i=1}^N f_k(u_{k-1}^\Delta(\tilde{z}_{k-1}^i, x), u_k^\Delta(\tilde{z}, x))} \right\} \tilde{q}_k(\tilde{z}, \tilde{z}') \lambda_{d_x}(d\tilde{z}') + \\ &\quad \delta_{\{\tilde{z}\}}(d\tilde{z}') \left[1 - \int_{\mathbb{R}^{d_x}} \min \left\{ 1, \frac{p_N(u_k^\Delta(\tilde{z}', \epsilon)) \frac{1}{N} \sum_{i=1}^N f_k(u_{k-1}^\Delta(\tilde{z}_{k-1}^i, x), u_k^\Delta(\tilde{z}', x))}{p_N(u_k^\Delta(\tilde{z}, \epsilon)) \frac{1}{N} \sum_{i=1}^N f_k(u_{k-1}^\Delta(\tilde{z}_{k-1}^i, x), u_k^\Delta(\tilde{z}, x))} \right\} \times \right. \\ &\quad \left. \tilde{q}_k(\tilde{z}, \tilde{z}') \lambda_{d_x}(d\tilde{z}') \right] \end{aligned}$$

where $\tilde{q}_k(\tilde{z}, \tilde{z}')$ is the Gaussian proposal density used at time k and $\delta_{\{z\}}(dz')$ is the Dirac measure on the set $\{z\}$. The case $k = 1$ is similar and is not written as it should be clear from the context. For $(\tilde{z}, \tilde{z}_{k-1}^1, \dots, \tilde{z}_{k-1}^N) \in \mathbb{R}^{(N+1)d_x}$ given and any $k \geq 2$ we write the conditional expectation, associated to K_k^Δ , of any $\varphi : \mathbb{R}^{d_x} \rightarrow \mathbb{R}$ that is bounded and measurable (write the collection of such functions $\mathcal{B}_b(\mathbb{R}^{d_x})$) as

$$\mathbb{E}_k^\Delta \left[\varphi(\tilde{z}') \middle| \tilde{z}, \tilde{z}_{k-1}^1, \dots, \tilde{z}_{k-1}^N \right] = \int_{\mathbb{R}^{d_x}} \varphi(\tilde{z}') K_k^\Delta(\tilde{z}, d\tilde{z}').$$

If $k = 1$ we simply write the expectation associated to K_1^Δ

$$\mathbb{E}_1^\Delta \left[\varphi(\tilde{z}') \middle| \tilde{z} \right].$$

In the degenerate case we can consider a sequence of random walk Metropolis kernels with Gaussian proposals in dimension $d_x - d_y$. Again, the MCMC kernel, $K_k^* : \mathbb{R}^{d_x - d_y} \times \mathcal{B}(\mathbb{R}^{d_x - d_y}) \rightarrow [0, 1]$, can be described at any time $k \geq 2$, for $(z_{k-1}^1, \dots, z_{k-1}^1) \in \mathbb{R}^{N(d_x - d_y)}$ given

$$\begin{aligned} K_k^*(z, dz') &= \min \left\{ 1, \frac{\frac{1}{N} \sum_{i=1}^N f_k(u_{k-1}^*(z_{k-1}^i), u_k^*(z'))}{\frac{1}{N} \sum_{i=1}^N f_k(u_{k-1}^*(z_{k-1}^i), u_k^*(z))} \right\} q_k(z, z') \lambda_{d_x - d_y}(dz') + \\ &\quad \delta_{\{z\}}(dz') \left[1 - \int_{\mathbb{R}^{d_x - d_y}} \min \left\{ 1, \frac{\frac{1}{N} \sum_{i=1}^N f_k(u_{k-1}^*(z_{k-1}^i), u_k^*(z'))}{\frac{1}{N} \sum_{i=1}^N f_k(u_{k-1}^*(z_{k-1}^i), u_k^*(z))} \right\} q_k(z, z') \lambda_{d_x - d_y}(dz') \right] \end{aligned}$$

where $q_k(z, z')$ is the Gaussian proposal density used at time k . Again, we do not explicitly write the case $k = 1$ as it should be fairly clear to the reader.

We are now ready to state our main result whose proof is in Appendix A.2. Recall that we use the notation $\tilde{z} = (z, \bar{z})^\top$.

Proposition 3.1. *For any $(\varphi, \tilde{z}) \in \mathcal{B}_b(\mathbb{R}^{d_x-d_y}) \times \mathbb{R}^{d_x}$ we have that*

$$\begin{aligned} \lim_{\Delta \downarrow 0} \mathbb{E}_1^\Delta \left[\varphi(Z') \middle| \tilde{z} \right] &= \int_{\mathbb{R}^{d_x}} \varphi(z') \min \left\{ 1, \frac{p_{\mathbb{N}}(\bar{z}') f_1(x_0, u_1^*(z'))}{p_{\mathbb{N}}(\bar{z}) f_1(x_0, u_1^*(z))} \right\} \tilde{q}_1(\tilde{z}, \tilde{z}') \lambda_{d_x}(d\tilde{z}') + \\ &\quad \varphi(z) \left[1 - \int_{\mathbb{R}^{d_x}} \min \left\{ 1, \frac{p_{\mathbb{N}}(\bar{z}') f_1(x_0, u_1^*(z'))}{p_{\mathbb{N}}(\bar{z}) f_1(x_0, u_1^*(z))} \right\} \tilde{q}_1(\tilde{z}, \tilde{z}') \lambda_{d_x}(d\tilde{z}') \right]. \end{aligned}$$

In addition, for any $(\varphi, k, N, \tilde{z}) \in \mathcal{B}_b(\mathbb{R}^{d_x-d_y}) \times \{2, 3, \dots\} \times \mathbb{N} \times \mathbb{R}^{d_x}$ and $(\tilde{z}_{k-1}^1, \dots, \tilde{z}_{k-1}^N) \in \mathbb{R}^{Nd_x}$ we have that

$$\begin{aligned} \lim_{\Delta \downarrow 0} \mathbb{E}_k^\Delta \left[\varphi(Z') \middle| \tilde{z}, \tilde{z}_{k-1}^1, \dots, \tilde{z}_{k-1}^N \right] &= \\ \int_{\mathbb{R}^{d_x}} \varphi(z') \min \left\{ 1, \frac{p_{\mathbb{N}}(\bar{z}') \frac{1}{N} \sum_{i=1}^N f_k(u_{k-1}^*(z_{k-1}^i), u_k^*(z'))}{p_{\mathbb{N}}(\bar{z}) \frac{1}{N} \sum_{i=1}^N f_k(u_{k-1}^*(z_{k-1}^i), u_k^*(z))} \right\} \tilde{q}_k(\tilde{z}, \tilde{z}') \lambda_{d_x}(d\tilde{z}') + \\ &\quad \varphi(z) \left[1 - \int_{\mathbb{R}^{d_x}} \min \left\{ 1, \frac{p_{\mathbb{N}}(\bar{z}') \frac{1}{N} \sum_{i=1}^N f_k(u_{k-1}^*(z_{k-1}^i), u_k^*(z'))}{p_{\mathbb{N}}(\bar{z}) \frac{1}{N} \sum_{i=1}^N f_k(u_{k-1}^*(z_{k-1}^i), u_k^*(z))} \right\} \tilde{q}_k(\tilde{z}, \tilde{z}') \lambda_{d_x}(d\tilde{z}') \right]. \end{aligned}$$

The result says, in our context, as we send the noise to zero, performing SMCMC on the low noise case converges to an SMCMC which, marginally, has an invariant measure that is the degenerate noise case. Indeed if one chose

$$\tilde{q}_k(\tilde{z}, \tilde{z}') = q_k(z, z') p_{\mathbb{N}}(\bar{z})$$

then, marginally, one would be using the kernel K_k^* in the limit as $\Delta \downarrow 0$. This result has important implications from the point of view of robustness of computational efficiency with decreasing Δ close to zero. If in the degenerate case K_k^* mixes well then one should expect good mixing when using SMCMC in the low noise case. As remarked previously, generic SMCMC without the methodology proposed in this paper can struggle to be efficient in the low noise case even when using sophisticated state of the art MCMC algorithms due to the conditional likelihood of Y_k given X_k being too informative.

4 Numerical Results

In this section we illustrate the performance of the proposed SMCMC method on four different examples. For brevity we will only consider only the degenerate noise case as this is the most challenging case. In the first example, we consider a moderate-dimensional linear Gaussian state-space model where the Kalman filter provides an analytical expression for the optimal solution. In the second example, we consider a Gaussian state-space model with a nonlinear observation function. In the third example, we have the Fitzhugh-Nagumo model, which is a low-dimensional diffusion model. Finally, we run our proposed method on a high-dimensional discretization of a certain stochastic partial differential equation (SPDE), namely the Kuramoto-Sivashinsky equation. Regarding assessing accuracy of our SMCMC method, for the first two examples there are tractable benchmarks and for the third and fourth examples we will use separate offline implementations of manifold Hamiltonian Monte Carlo (HMC) in [15] for a selection of time values. We note that HMC as an MCMC algorithm is intrinsically not suitable for filtering as its computational cost for n observation times is $\mathcal{O}(n^2)$. Still it can serve as a reliable benchmark here despite being expensive due to its suitability for problems defined on manifolds.

4.1 Linear Gaussian Model

Let us consider the linear Gaussian state-space model:

$$\begin{aligned} Y_k &= AX_k \\ X_k &= BX_{k-1} + C\nu_k, \quad \nu_k \sim \mathcal{N}(0, \mathbb{I}_{d_x}) \end{aligned}$$

where $X_k \in \mathbb{R}^{d_x}$ is the state vector, $Y_k \in \mathbb{R}^{d_y}$ is the observation vector ($d_y < d_x$), $A \in \mathbb{R}^{d_y \times d_x}$ is the observation matrix, $B \in \mathbb{R}^{d_x \times d_x}$ is the state transition matrix, $C \in \mathbb{R}^{d_y \times d_x}$ is the noise coefficient matrix and ν_k is the noise with covariance \mathbb{I}_{d_x} for $k \in \{1, \dots, n\}$. We fix the dimensions of the problem to $d_y = 1$, $d_x = 20$ and $n = 30$ observations. We set $A = [1, 0, \dots, 0]$ so that the observation corresponds to the first component of the state vector, $B = \mathbf{1}_{d_x \times d_x}/d_x$ (where $\mathbf{1}_{d_x \times d_x}$ is the square matrix of ones) which is equivalent to averaging the state, and $C = \sigma \mathbb{I}_{d_x}$ with $\sigma = 0.1$. The initial state X_0 is assumed to be fixed and equal to zero. The Kalman filter provides the optimal solution for this model, which we use as a benchmark to evaluate the performance of our proposed method.

We run the SMCMC algorithm from Section 3.3 with $\rho = 0.05$ tuned to achieve an acceptance rate of approximately 0.234. We set $N = 10^4$ and $s = 20$. We report the acceptance rate and effective sample size (ESS) of the SMCMC runs at each time step $k \in \{1, 2, \dots, n\}$ in Figure 1. The acceptance rates stay consistent across time steps and the ESS is around 100-200. The ESS per second is around 50-100, which might be expected from a random walk Metropolis-Hastings algorithm with isotropic proposals in moderate dimensions, but could be improved with adapted correlated proposals or more advanced MCMC methods.

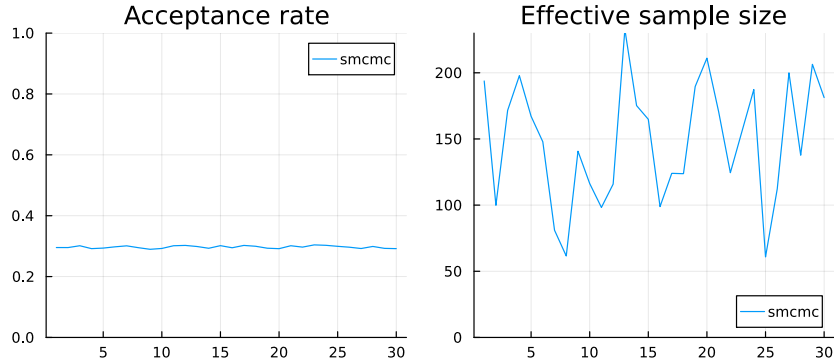


Figure 1: Linear Gaussian Model. Acceptance rate (left) and effective sample size (right) of the SMCMC sampler against time index.

If we look at the marginals of the second component $X_{k,2}$ at time steps $k \in \{5, 10, 15, 20, 25, 30\}$ displayed in Figure 2, we can see that the kernel density estimate (KDE) of the SMCMC samples (blue) matches the Kalman filter (black) well. The fit is not perfect, due to low ESS, but the overall shape of the distribution is captured well. One can improve the fit by increasing the number of samples N , as well as the size s of the conditioning set, at the cost of increased computing time (lower ESS per second).

On the Choice of the s Parameter

We now investigate the effect of the choice of the s parameter in the SMCMC algorithm. For this linear Gaussian model we run the SMCMC algorithm with different values of $s \in \{1, 10, 20, 30, 40, 50\}$. We set $N = 10^4$ and set the stepsize to 0.05 which yields the same acceptance rate of approximately 0.234. We report the ESS, the L_2 error norm of the mean and standard deviation, and the total run time against different choices of s in Figure 3. As we can see, increasing s improves the ESS and the accuracy of the estimates, but also increases the computation time. The ESS seems to plateau after $s = 30$, while the error norms continue to decrease slightly. Therefore, there is a trade-off between accuracy and computational

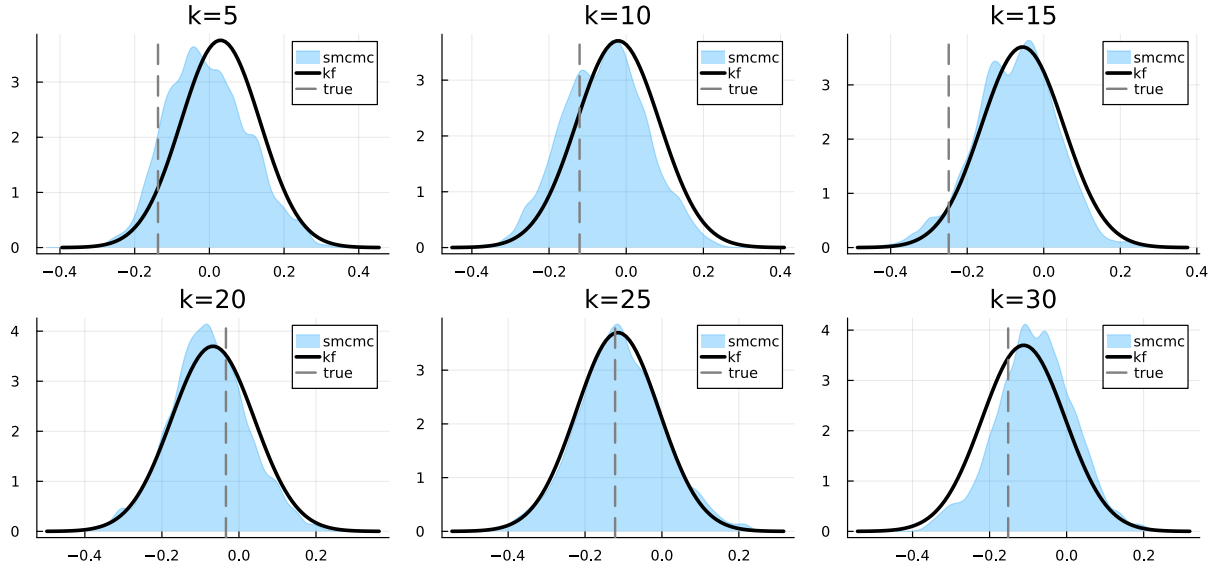


Figure 2: Linear Gaussian Model. Marginal posterior distributions of the second component $X_{k,2}$ at time steps $k \in \{5, 10, 15, 20, 25, 30\}$. The kernel density estimate of the SMC-MC samples is shown in blue and the Kalman filter is shown in black. The vertical dashed line indicates the true value of $X_{k,2}$ used to generate the observations.

cost when choosing the s parameter. A moderate value of s around 20-30 seems to provide a good balance between these two aspects, at least in this example. We see that our choice of $s = 20$ in previous experiments was reasonable.

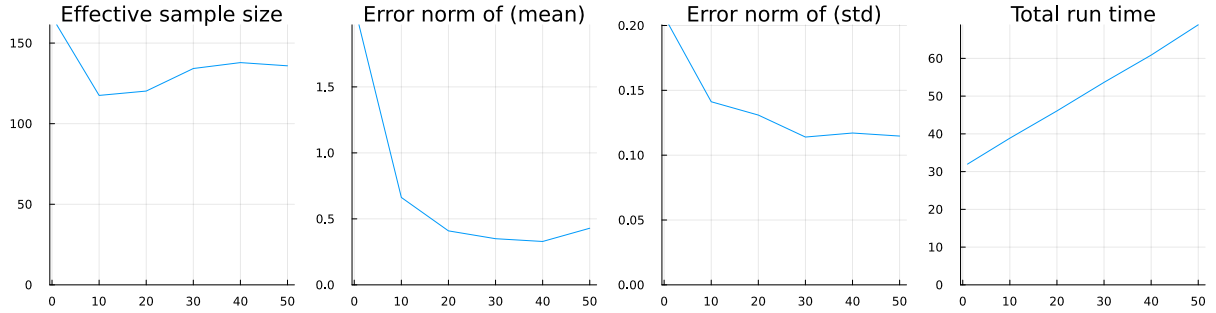


Figure 3: ESS, L_2 error norm of the mean and standard deviation, total run time against different choices of $s \in \{1, 10, 20, 30, 40, 50\}$ parameter (x-axis) in the linear Gaussian model.

4.2 Gaussian Model with Nonlinear Observations

We now consider a Gaussian state-space model with nonlinear observations:

$$\begin{aligned} Y_k &= h(X_k) \\ X_k &= BX_{k-1} + C\nu_k, \quad \nu_k \sim \mathcal{N}(0, \mathbb{I}_{d_x}) \end{aligned}$$

where $h : \mathbb{R}^{d_x} \rightarrow \mathbb{R}^{d_y}$ is a nonlinear function. We choose $h(X_k) = \|X_k\|^2$, that is, the manifold is a sphere. We set $d_y = 1$, $d_x = 100$ and use $n = 10$ observations. The state transition matrix is $B = 0.5\mathbb{I}_{d_x}$ and the noise coefficient matrix is $C = \mathbb{I}_{d_x}$ with $\sigma = 0.5$. The initial state X_0 is assumed to be fixed and equal to

zero. This choice introduces nonlinearity in the observations while keeping the model relatively simple. We can quickly check if the SMCMC sampler is correct by looking at the marginals at time step $k = 1$, which must be uniform on the sphere of radius $\sqrt{Y_1}$. We run the SMCMC algorithm with $\rho = 0.3$ tuned to achieve an acceptance rate of approximately 0.234. We set $N = 10^4$ and $s = 20$. We report the marginals of $X_{1,1}$, $X_{1,26}$, $X_{1,51}$ and $X_{1,76}$ at time step $k = 1$ in Figure 4. The KDE of the SMCMC samples (blue) matches the exact closed form distribution (black) well, indicating that the sampler is working correctly.

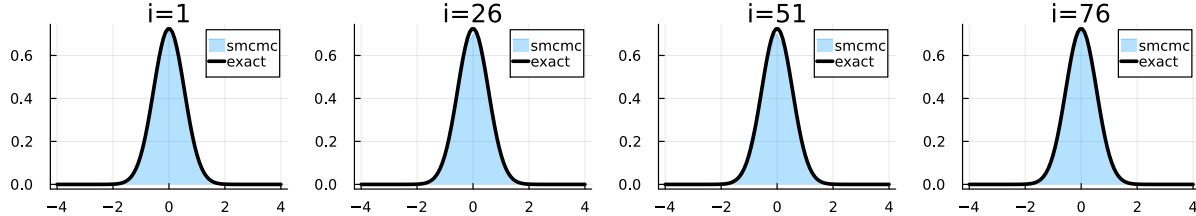


Figure 4: Gaussian Model with Nonlinear Observations. Marginal posterior distributions of $X_{1,1}$, $X_{1,26}$, $X_{1,51}$ and $X_{1,76}$ at time step $k = 1$. The kernel density estimates of the SMCMC samples are shown in blue and the exact marginals are shown in black.

4.3 FitzHugh-Nagumo Model

In our third example, we consider the FitzHugh-Nagumo (FHN) model, which is a hypoelliptic diffusion process modelling the spiking behavior of neurons. The model is given by the following system of stochastic differential equations (SDEs):

$$dX_t = a(X_t)dt + Bd\mathcal{W}_t$$

or more explicitly,

$$\begin{bmatrix} dX_1(t) \\ dX_2(t) \end{bmatrix} = \begin{bmatrix} \epsilon^{-1}(X_1(t) - X_1(t)^3 - X_2(t)) \\ \gamma X_1(t) - X_2(t) + \beta \end{bmatrix} dt + \begin{bmatrix} 0 \\ \sigma \end{bmatrix} d\mathcal{W}(t)$$

where the state vector is $X_t = (X_1(t), X_2(t))^\top \in \mathbb{R}^2$, and we assume that the diffusion matrix B is constant w.r.t. the state X_t . Here, $X_1(t)$ represents the membrane potential of the neuron and $X_2(t)$ is a recovery variable, which interacts nonlinearly in the drift term $a(X_t)$. The parameter ϵ controls the timescale separation between the fast variable $X_1(t)$ and the slow variable $X_2(t)$, while γ and β determine the shape of the dynamics and the external forcing. The parameter σ scales the intensity of the scalar Wiener noise process $d\mathcal{W}(t)$, which introduces stochasticity into the recovery variable and models random fluctuations in the system.

We discretize the SDE using a strong order 1.5 Taylor scheme, with the following update equations:

$$\begin{aligned} X_k = X_{k-1} + \delta a_{k-1} + \frac{1}{2} \delta^2 \partial a_{k-1} a_{k-1} + \frac{1}{4} \delta^4 [(\text{tr}(\partial^2 a_{k-1} B B^\top))_{i=0}^{d_x}] \\ + \delta^{1/2} B W_{k,1} + \frac{1}{2} \delta^{3/2} \partial a_{k-1} B (W_{k,1} + W_{k,2}/\sqrt{3}) \end{aligned}$$

where $a_{k-1} = a(X_{k-1})$ is a shorthand for the drift, ∂a_{k-1} is its Jacobian and $\partial^2 a_{k-1}$ its Hessian evaluated at $X_{k-1} = (X_1(t_k), X_2(t_k))^\top$, respectively, for a set of time discretization points $\{t_1, \dots, t_n\}$ that are δ distance apart. The vector $W_k = (W_{k,1}, W_{k,2})^\top \sim \mathcal{N}_2(0, I_2)$ is a 2-dimensional standard normal noise vector. To simulate from the model, we use the following parameters: $\sigma = 0.5$, $\epsilon = 0.2$, $\gamma = 1.5$, $\beta = 0.5$, $\delta = 0.05$ and $n = 100$ time steps. The initial state X_0 is set to zero. Such choices seem to produce stable dynamics. We observe the first component of the state at each time step with no noise. The simulated dataset is shown in Figure 5.

We run the SMCMC algorithm on this model and compare the results with the manifold HMC of [15]. Since the HMC produces samples from the joint posterior density, we run it separately for increasing state

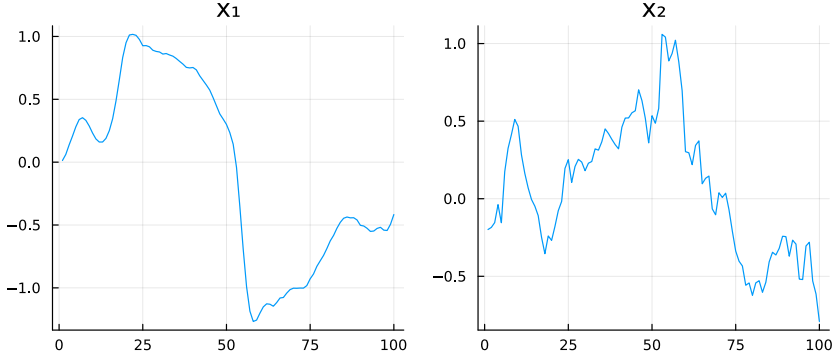


Figure 5: FHN Model. Observed (left) and hidden (right) components of the state over time.

space sizes, that is, for $X_1, X_{1:2}, \dots, X_{1:k}, \dots, X_{1:n}$. Then we select only the last state X_k from each run to compare with the SMCMC results. We run HMC for 750 iterations with 250 burn-in samples using the `mici` python library, which is a NUTS implementation for constrained sampling. For SMCMC, we run $N = 10^4$ iterations with the step-size tuned to yield 0.234 acceptance rate. We use a conditioning set of size $s = 20$. We present the acceptance rate and ESS of the SMCMC algorithm for each filtering target at $k \in \{1, 2, \dots, n\}$ in Figure 6. As we see, SMCMC has stable acceptance rate that is close to 0.2 with ESS being around 1000-1500. While SMCMC produces ESS that is lower than the actual sample size, due to antithetic properties the ESS from HMC is double the number of iterations. HMC adapted to the acceptance rate of 0.8 gives us 1500 effective samples (not shown). We have also timed the two algorithms to compare their efficiency. HMC produced up to 1000 effective samples per second for small n , around 150 for moderate n and about 50 for $n = 100$. The ESS per second for the HMC algorithm was computed by dividing the ESS of the k -th filtering samples by the running time of the main non-adaptive sampling stage. The latter runs have more parameters to sample, hence the decreasing trend. On the other hand, SMCMC produces about 250 effective samples per second, but the number is constant in time.

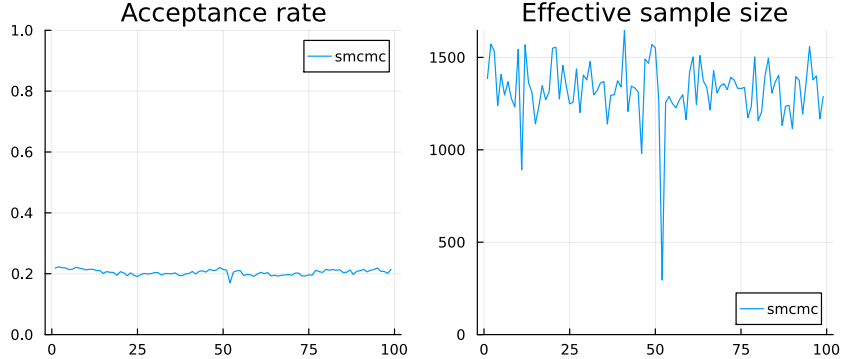


Figure 6: FHN Model. Acceptance rate (left) and ESS (right) of the SMCMC sampler against time index.

To confirm that we are sampling from the correct posterior, we look at the time marginals of $X_2(t_k)$ at time steps $k \in \{6, 19, 32, 45, 58, 71, 84, 97\}$. In Figure 7 we see that the SMCMC samples (in blue) match well the ones obtained from 8 separate runs of HMC (in orange and each for a different value of k).

4.4 Kuramoto-Sivashinsky Equation

We now consider a high-dimensional filtering problem arising from a discretized stochastic partial differential equation (SPDE), the Kuramoto-Sivashinsky (KS) equation. The KS equation is a fourth-order

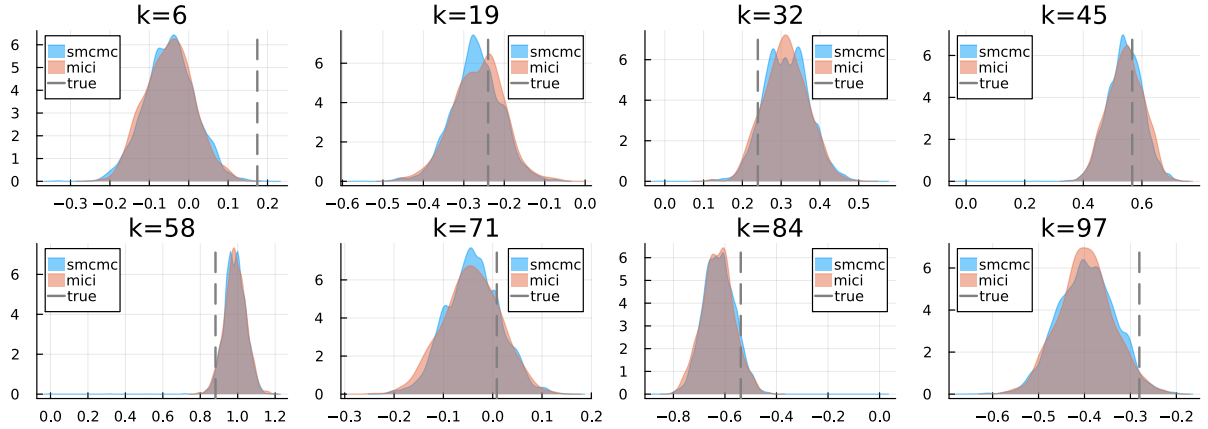


Figure 7: FHN Model. Marginal posterior distributions of the second component $X_2(t_k)$ at time steps $k \in \{6, 19, 32, 45, 58, 71, 84, 97\}$. The SMCMC samples are shown in blue and the HMC results are shown in orange (and displayed in the captions as mici). The vertical dotted lines display the value of the true signal used to generate the data.

nonlinear SPDE that describes the diffusive instabilities in a laminar flame front, and is given by:

$$\frac{d}{dt}X(\mathbf{s}, t) + \frac{\partial^2}{\partial \mathbf{s}^2}X(\mathbf{s}, t) + \frac{\partial^4}{\partial \mathbf{s}^4}X(\mathbf{s}, t) + X(\mathbf{s}, t)\frac{\partial}{\partial \mathbf{s}}X(\mathbf{s}, t) + \gamma X(\mathbf{s}, t) = \frac{d}{dt}\mathcal{W}(\mathbf{s}, t)$$

The state variable $X(\mathbf{s}, t)$ represents the amplitude of the flame front at position \mathbf{s} and time t , γ is a damping parameter, and $\mathcal{W}(\mathbf{s}, t)$ is a space-time white noise process that is white in time and correlated in space. The equation is defined on a spatial domain $\mathbf{s} \in [0, S]$ with periodic boundary conditions. The system can be discretized in space using a finite difference method with d_x grid points. In the time direction we use an implicit-explicit Euler scheme to handle the stiff linear terms and the nonlinear term separately. The discretized state-space model is given by:

$$\begin{aligned} \frac{X_{k,i} - X_{k-1,i}}{\delta_t} + \frac{X_{k,i+1} - 2X_{k,i} + X_{k,i-1}}{\delta_s^2} + \frac{X_{k,i+2} - 4X_{k,i+1} + 6X_{k,i} - 4X_{k,i-1} + X_{k,i-2}}{\delta_s^4} \\ + X_{k-1,i} \frac{X_{k-1,i+1} - X_{k-1,i-1}}{2\delta_s} + \gamma X_{k,i} = \frac{\mathcal{W}_{k,i} - \mathcal{W}_{k-1,i}}{\sqrt{\delta_t}} \end{aligned}$$

where we set $X_{k,i} = X(\mathbf{s}_i, t_k)$, $\mathcal{W}_{k,i} = \mathcal{W}(\mathbf{s}_i, t_k)$, $\mathbf{s}_i - \mathbf{s}_{i-1} = \delta_s$, $t_k - t_{k-1} = \delta_t$ for $i = 1, \dots, d_x$, $k \in \{1, \dots, n\}$. For the noise increments let $\nu_{k,i} = \mathcal{W}_{k,i} - \mathcal{W}_{k-1,i}$ and the vector $\nu_k = (\nu_{k,1}, \dots, \nu_{k,d_x})^\top$ is assumed to be independent in time k and correlated in space with covariance matrix $\Sigma = LL^\top$, that is, $\nu_k \sim \mathcal{N}(0, \Sigma)$. Now we can rearrange the terms to obtain the state transition equation:

$$\left((1 + \gamma)\mathbf{I} + \frac{\delta_t}{\delta_s^2}D_2 + \frac{\delta_t}{\delta_s^4}D_4 \right) X_k = X_{k-1} - X_{k-1} \odot \left(\frac{\delta_t}{2\delta_s}D_1 \right) X_{k-1} + \left(\delta_t^{1/2}L \right) \nu_k$$

where D_1 , D_2 and D_4 are the matrices of finite difference coefficients for the first, second and fourth derivatives with periodic boundary conditions, respectively, \odot denotes the element-wise product and \mathbf{I} is the identity matrix. This is simplified to

$$X_k = A^{-1} (X_{k-1} - X_{k-1} \odot BX_{k-1}) + A^{-1}C\nu_k$$

where $A = (1 + \gamma)\mathbf{I} + \frac{\delta_t}{\delta_s^2}D_2 + \frac{\delta_t}{\delta_s^4}D_4$, $B = \frac{\delta_t}{2\delta_s}D_1$ and $C = \delta_t^{1/2}L$. We assume a continuous observation model, where we observe certain components of the state vector at each time step:

$$Y_k = HX_k$$

where $H = [e_1, e_{1+l}, e_{1+2l}, \dots]^\top$ has rows that are the standard basis vectors e_i selecting every l -th component of the state vector.

To simulate the dynamics, we set the dimensions to $d_t = 100$, $d_x = 100$, $d_y = 10$ (i.e. $l = 10$), and parameters to $S = 10\pi$, $\gamma = 0.01$, $\delta_s = S/d_x$, $\delta_t = \delta_s^2/2$. The covariance matrix is constructed using the Matérn covariance function with smoothness $\alpha = 1/2$, range $r = 10$ and marginal variance $\sigma^2 = 2.0^2$. The initial state is set to $X_0 = X(s, t = 0) = 3/2 \times \cos(s/5)$, $s \in [0, S]$. The simulated dataset is shown in Figure 8. We can see that the realized dynamics exhibit chaotic behavior, which we achieve by using a large spatial domain $[0, S]$ and a small damping parameter γ . In Figure 9, one can find the L_2 norm of

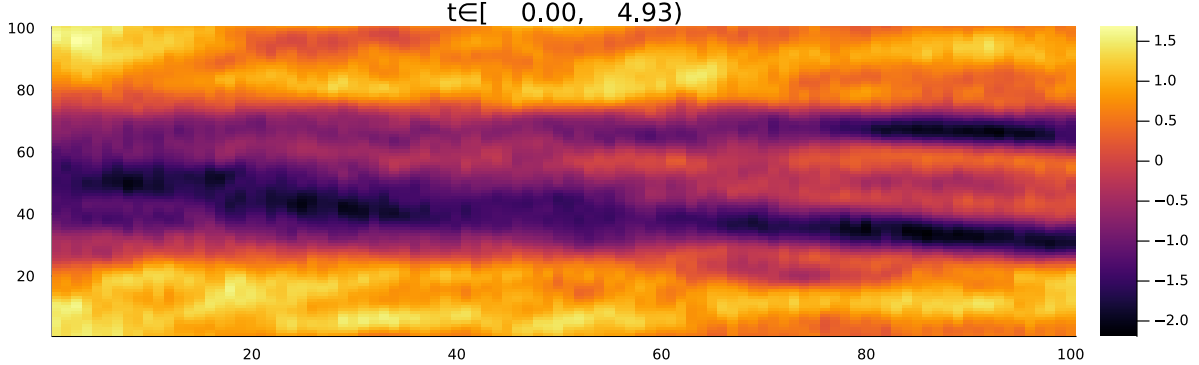


Figure 8: Simulated data from the KS equation. The x-axis represents the temporal dimension and the y-axis represents the spatial dimension.

the state across time and possible realizations of X_k at $k = 81$. The norm is contained within the range of $(0, 12)$ and does not blow up as the dynamic evolves. This is because the friction term acts as a damper by reducing the energy of the system, which would otherwise keep increasing as we add the noise. The spatial variation is smooth with long range correlations, as expected by our Matérn covariance structure.

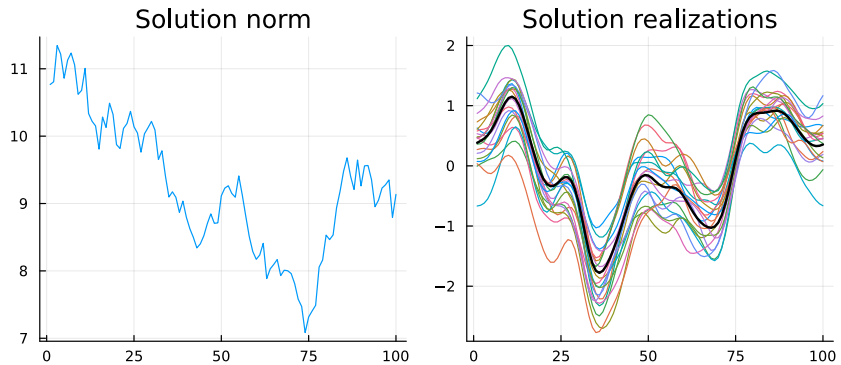


Figure 9: KS Model. L_2 norm of the state across time (left) and possible realizations of X_k at $k = 81$ (right).

For this model we run the SMCMC algorithm for the full data, whereas, due to computational limitations, we run HMC only for certain time-indices. For HMC the overall setup is identical with the previous example: we run 250 steps for adaptation and 750 main iterations, but we run HMC only for $k \in \{2, 16, 30, 44, 58, 72, 86, 100\}$ (separately). To improve the mixing of our own MCMC kernel, we precondition the state via the change of variables $V_k = P^{-1}X_k$. Here, P is the Cholesky factor of the covariance of the conditional law $X_k|Y_k, X_{k-1}$ of the noisy observation model. That is, if $Y_k|X_k \sim \mathcal{N}(HX_k, R)$ with $R = \sigma_y^2 \mathbb{I}$, then $X_k|Y_k, X_{k-1} \sim \mathcal{N}(\mu_k, \Sigma_k)$ with $\Sigma_k = (A^{-1}C\Sigma C^\top A^{-\top} + H^\top R^{-1}H)^{-1}$

and $\mu_k = \Sigma_k(A^{-1}(X_{k-1} - X_{k-1} \odot BX_{k-1}) + H^\top R^{-1}Y_k)$. The preconditioning is equivalent to using the metric tensor $M_k = \Sigma_k^{-1}$ in the Riemannian manifold MCMC kernel. We run SMCMC for $N = 2 \times 10^4$ samples with step-size tuned to achieve 0.234 acceptance rate and conditioning set size $s = 20$. The results are shown in Figure 10. The acceptance rate is stable across time steps, around 0.234. The median ESS is around 60, which is reasonable for a random walk Metropolis-Hastings algorithm in high dimensions. The ESS per second is quite low, around 3 samples per second, but the dimension of the problem is larger compared to previous examples.

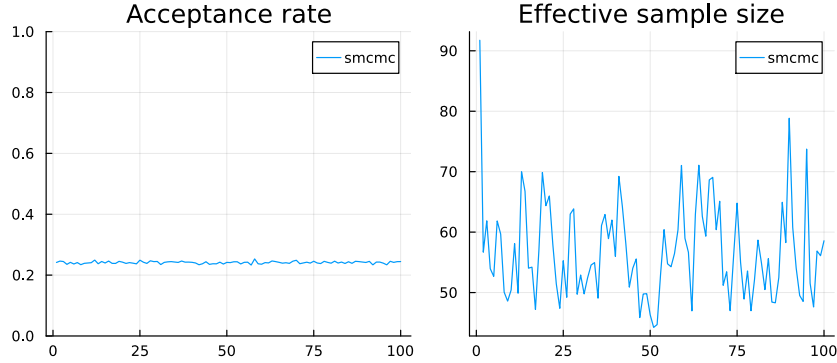


Figure 10: KS Model. Acceptance rate (left) and ESS (right) of the SMCMC sampler against time index.

Due to the large size of the problem (10^4 parameters in total), we could not run the joint HMC for every filtering target. The eight runs we have conducted for HMC already exceeded the 20 hour time mark. Running more iterations and chains for the selected time steps would be computationally challenging, and even more so for all time steps. With these benchmarks we chose to compare the mean of the filter obtained from SMCMC and HMC at these time steps. In Figure 11, we look at the estimated mean of the field at time steps $k \in \{2, 16, 30, 44, 58, 72, 86, 100\}$. The SMCMC results (blue) seem to align with the HMC results (orange) and with the true hidden state (black). The L_2 error norm of the estimates from the two methods is reported in Table 1. Both methods yield comparable results. Overall, the results suggest that the SMCMC method is able to capture the filtering distribution reasonably well, even in this high-dimensional and complex setting.

Table 1: L_2 error norms of the mean estimates at time steps $k \in \{2, 16, 30, 44, 58, 72, 86, 100\}$.

Time step	2	16	30	44	58	72	86	100
SMCMC	1.144	2.454	1.721	2.217	2.71	2.425	1.735	1.151
HMC	0.808	1.285	1.791	1.893	2.375	1.923	3.681	2.111

Acknowledgements

AZ & AJ were supported by CUHK-SZ start up funding.

A Proofs

A.1 Proof of Proposition 2.1

Proof. For the case of the filter at time 1, we can just apply [12, Proposition 2(b)] along with the equivalence of the Riemannian and Hausdorff measure (e.g. [15, Lemma C.2.]). For $k \geq 2$ we recall that the filter is the time k marginal of the smoother at time k . We will find the density of the smoother

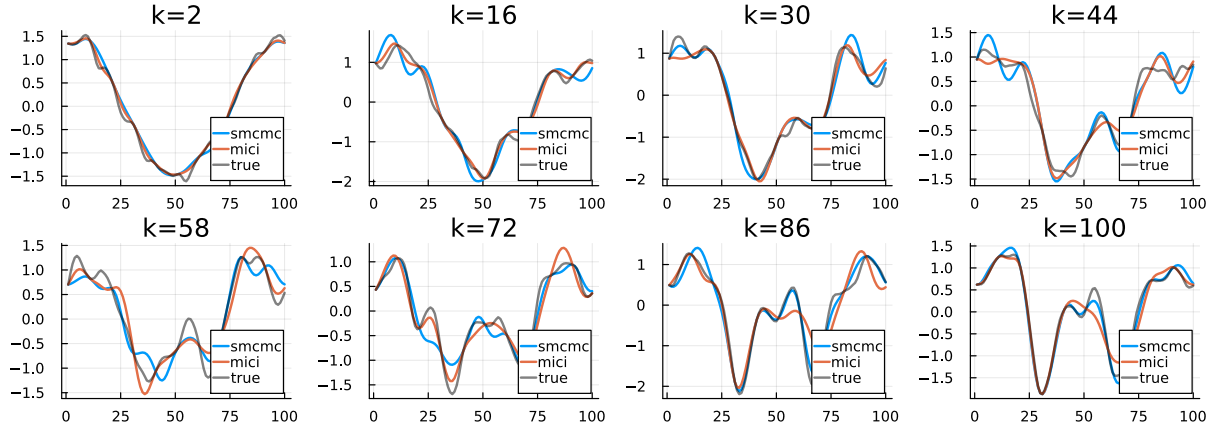


Figure 11: Mean estimates of the field X_k at time steps $k \in \{2, 16, 30, 44, 58, 72, 86, 100\}$.

$\pi_k(x_{1:k})$ w.r.t. $\sigma_{\mathbf{M}_k}^{\mathbf{M}_k}$. Applying again [12, Proposition 2(b)] along with the equivalence of the Riemannian and Hausdorff measure

$$\pi_k(x_{1:k}) \propto \det(\partial \mathbf{c}_k(x_{1:k}) \mathbf{M}_k^{-1} \partial \mathbf{c}_k(x_k)^\top)^{-1/2} \prod_{s=1}^k f_s(x_{s-1}, x_s).$$

Then due to the block structure of $\partial \mathbf{c}_k$ and \mathbf{M}_k we have

$$\det(\partial \mathbf{c}_k(x_{1:k}) \mathbf{M}_k^{-1} \partial \mathbf{c}_k(x_k)^\top)^{-1/2} = \prod_{s=1}^k g_s(x_s)$$

and by standard properties of the Riemannian measure $\mu_{\mathbf{M}_k}^{\mathbf{M}_k} = \bigotimes_{s=1}^k \sigma_{\mathbf{M}_s}^{M_s}$.

As a result of the above arguments, we have that

$$\begin{aligned} \pi_k(x_k) &= \frac{g_k(x_k) \int_{\mathbf{M}_{k-1}} f(x_{k-1}, x_k) \prod_{s=1}^{k-1} g_s(x_s) f_s(x_{s-1}, x_s) \bigotimes_{s=1}^{k-1} \sigma_{\mathbf{M}_s}^{M_s}(dx_s)}{\int_{\mathbf{M}_k} \prod_{s=1}^k g_s(x_s) f_s(x_{s-1}, x_s) \bigotimes_{s=1}^{k-1} \sigma_{\mathbf{M}_s}^{M_s}(dx_s)} \\ &= g_k(x_k) \int_{\mathbf{M}_{k-1}} f(x_{k-1}, x_k) \left\{ \int_{\mathbf{M}_{k-2}} \prod_{s=1}^{k-1} g_s(x_s) f_s(x_{s-1}, x_s) \bigotimes_{s=1}^{k-2} \sigma_{\mathbf{M}_s}^{M_s}(dx_s) \right\} \sigma_{\mathbf{M}_{k-1}}^{M_{k-1}}(dx_{k-1}) \times \\ &\quad \left(\int_{\mathbf{M}_k} \left[g_k(x_k) \int_{\mathbf{M}_{k-1}} f(x_{k-1}, x_k) \left\{ \int_{\mathbf{M}_{k-2}} \prod_{s=1}^{k-1} g_s(x_s) f_s(x_{s-1}, x_s) \bigotimes_{s=1}^{k-2} \sigma_{\mathbf{M}_s}^{M_s}(dx_s) \right\} \right] \sigma_{\mathbf{M}_{k-1}}^{M_{k-1}}(dx_{k-1}) \right)^{-1} \\ &= \frac{g_k(x_k) \int_{\mathbf{M}_{k-1}} f_k(x_{k-1}, x_k) \pi_{k-1}(x_{k-1}) \sigma_{\mathbf{M}_{k-1}}^{M_{k-1}}(dx_{k-1})}{\int_{\mathbf{M}_k} g_k(x_k) \int_{\mathbf{M}_{k-1}} f_k(x_{k-1}, x_k) \pi_{k-1}(x_{k-1}) \sigma_{\mathbf{M}_{k-1}}^{M_{k-1}}(dx_{k-1}) \sigma_{\mathbf{M}_k}^{M_k}(dx_k)} \end{aligned}$$

where we have divided by

$$\int_{\mathbf{M}_{k-1}} \prod_{s=1}^{k-1} g_s(x_s) f_s(x_{s-1}, x_s) \bigotimes_{s=1}^{k-1} \sigma_{\mathbf{M}_s}^{M_s}(dx_s)$$

in the numerator and denominator to move from the second to the third line. \square

A.2 Proof of Proposition 3.1

Proof. We consider the case $k \geq 2$ as the case $k = 1$ follows in a similar manner and we only give the proof when considering acceptance part of the kernel as the proof for the rejection part will follow in almost the same way. In other words we are considering what happens to

$$\int_{\mathbb{R}^{d_x}} \varphi(z') \min \left\{ 1, \frac{p_{\mathbb{N}}(u_k^\Delta(\tilde{z}', \epsilon)) \frac{1}{N} \sum_{i=1}^N f_k(u_{k-1}^\Delta(\tilde{z}_{k-1}^i, x), u_k^\Delta(\tilde{z}', x))}{p_{\mathbb{N}}(u_k^\Delta(\tilde{z}, \epsilon)) \frac{1}{N} \sum_{i=1}^N f_k(u_{k-1}^\Delta(\tilde{z}_{k-1}^i, x), u_k^\Delta(\tilde{z}, x))} \right\} \tilde{q}_k(\tilde{z}, \tilde{z}') \lambda_{d_x}(d\tilde{z}').$$

As $\Delta \downarrow 0$ we have that for any $\tilde{z} \in \mathbb{R}^{d_x}$ (recall $z = (z, \bar{z})^\top$)

$$u_k^\Delta(\tilde{z}) \rightarrow \begin{bmatrix} z_k^* \\ 0 \end{bmatrix} + \begin{bmatrix} V_k^* z \\ \bar{z} \end{bmatrix}$$

this is because

$$V_k^\Delta \rightarrow \begin{bmatrix} V_k^* & 0 \\ 0 & \mathbb{I}_{d_y} \end{bmatrix}.$$

Therefore we have that

$$\begin{aligned} \min \left\{ 1, \frac{p_{\mathbb{N}}(u_k^\Delta(\tilde{z}', \epsilon)) \frac{1}{N} \sum_{i=1}^N f_k(u_{k-1}^\Delta(\tilde{z}_{k-1}^i, x), u_k^\Delta(\tilde{z}', x))}{p_{\mathbb{N}}(u_k^\Delta(\tilde{z}, \epsilon)) \frac{1}{N} \sum_{i=1}^N f_k(u_{k-1}^\Delta(\tilde{z}_{k-1}^i, x), u_k^\Delta(\tilde{z}, x))} \right\} \rightarrow \\ \min \left\{ 1, \frac{p_{\mathbb{N}}(\tilde{z}') \frac{1}{N} \sum_{i=1}^N f_k(u_{k-1}^*(z_{k-1}^i), u_k^*(z'))}{p_{\mathbb{N}}(\tilde{z}) \frac{1}{N} \sum_{i=1}^N f_k(u_{k-1}^*(z_{k-1}^i), u_k^*(z))} \right\}. \end{aligned}$$

The proof is then concluded via dominated convergence. \square

References

- [1] ANDRIEU, C., DOUCET, A. & HOLENSTEIN, R. (2010). Particle Markov chain Monte Carlo methods (with discussion). *J. R. Statist. Soc. Ser. B*, **72**, 269–342.
- [2] BAIN, A., & CRISAN, D. (2009). *Fundamentals of Stochastic Filtering*. Springer: New York.
- [3] BARCZYK, M. BONNABEL, S., DESCHAUD, J. & GOULETTE, F. (2015). Invariant EKF design for scan matching-aided localization. *IEEE Trans. Control Syst. Technol.*, **23**, 2440-2448.
- [4] BERZUINI, C., BEST, N. G., GILKS, W. R. & LARIZZA, C. (1997). Dynamic conditional independence models and Markov chain Monte Carlo methods. *J. Amer. Statist. Soc.*, **92**, 1403-1412.
- [5] BESKOS, A., CRISAN, D., JASRA, A., KAMATANI, K., & ZHOU, Y. (2017). A stable particle filter for a class of high-dimensional state-space models. *Adv. Appl. Probab.*, **49**, 24–48.
- [6] BHARATH, K., LEWIS, A., SHARMA, A. TRETYAKOV, M. (2025). Sampling and Estimation on Manifolds using the Langevin Diffusion. *J. Mach. Learn. Res.* (to appear).
- [7] BRIGO, D. (1996). New results on the Gaussian projection filter with small observation noise. *Systems & control letters*, **28** (5), 273-279.
- [8] BYRNE, S. & GIROLAMI, M. (2013). Geodesic Monte Carlo on embedded manifolds. *Scand. J. Stat.* **40**, 825–845.
- [9] CENTANNI, S. & MINOZZO, M. (2006). A Monte Carlo approach to filtering for a class of marked doubly stochastic Poisson processes. *J. Amer. Stat. Ass.*, **101**, 1582-1597.

[10] CRISAN, D., KOURITZIN, M. & XIONG, J. (2009). Nonlinear filtering with signal dependent observation noise. *Elec. J. Probab.*, **63**, 1863–1883.

[11] DEL MORAL, P. (2004). *Feynman-Kac Formulae: Genealogical and Interacting Particle Systems with Applications*. Springer: New York.

[12] DIACONIS, P. HOLMES, S. & SHAHSHAHANI, M. (2013). Sampling from a manifold. In *Advances in Modern Statistical Theory and Applications: A Festschrift in honor of Morris L. Eaton* (eds G. Jones & X. Shen), IMS.

[13] ESCUDERO, M. C. (2024). *Approximate Manifold Sampling*. PhD Thesis, University of Bristol.

[14] GRAHAM, M., & STORKEY, A. (2017). Asymptotically exact inference in differentiable generative models. *Elec. J. Stat.*, **11**, 5105–5164.

[15] GRAHAM, M., THIERY, A. & BESKOS, A. (2022). Manifold Markov chain Monte Carlo methods for Bayesian inference in diffusion models, *J. R. Statist. Soc. B*, **84**, 1229-1256.

[16] HIJAB, O. (1981) Asymptotic Bayesian Estimation of a First Order Equation with Small Diffusion. *Ann. Probab.*, **12** (3) 890 – 902.

[17] HUA, A., DUCARD, G., HAMEL, T. MAHONY, R. & RUDIN, K. (2014). Implementation of a nonlinear attitude estimator for aerial robotic vehicles. *IEEE Trans. Control Syst. Technol.*, **22**, 201-213.

[18] JOANNIDES, M. & LEGLAND, F. (1997). Nonlinear filtering with perfect discrete time observations. *Proc. 34th IEEE Conf. Dec. Control*, 4012-4017.

[19] KANTAS, N., BESKOS, A. & JASRA, A. (2014). Sequential Monte Carlo for inverse problems: a case study for Navier Stokes. *SIAM/ASA JUQ*, **2**, 464-489.

[20] KATZUR, R., BOBROVSKY, B.Z., and SCHUSS, Z. (1984) Asymptotic analysis of the optimal filtering problem for one-dimensional diffusions measured in a low noise channel, Part I and II, *SIAM J. Appl. Math.*, **44**, pp. 591-604, and pp. 1176-1191.

[21] KUTOYANTS, Y. A. (2025). Extended adaptive Kalman filter with low noise observations. *Probability, Uncertainty and Quantitative Risk*.

[22] MARTIN, J. S., JASRA, A., & MCCOY, E. (2013). Inference for a class of partially observed point process models. *Ann. Inst. Stat. Math.*, **65**, 413–437.

[23] MILHEIRO DE OLIVEIRA, P. (1994) Approximate filters for a nonlinear discrete time filtering problem with small observation noise, *Stochastics and Stochastic Reports*, **46**(1-2): 1–24.

[24] MURRAY, L.M., JONES, E.M. & PARSLOW, J. (2013). On disturbance state-space models and the particle marginal Metropolis-Hastings sampler. *SIAM/ASA JUQ*, **1**, 494-521.

[25] PARDOUX, E., & ZEITOUNI, O. (2004). Quenched large deviations for one dimensional nonlinear filtering. *SIAM Journal on Control and Optimization*, **43** (4), 1272–1297.

[26] PICARD, J. (1986) Nonlinear filtering of one-dimensional diffusion in the case of a high signal-to-noise ratio, *SIAM Journal on Applied Mathematics*, **46**(6): 1098–1125.

[27] PICARD, J. (1991) Efficiency of the extended Kalman filter for nonlinear systems with small noise, *SIAM Journal on Applied Mathematics*, **51**(4): 843–885.

[28] RUZAYQAT, H. , ER-RAIY, A., BESKOS, A., CRISAN, D. , JASRA, A. & KANTAS, N. (2022). A lagged particle filter in high-dimensions. *SIAM/ASA JUQ* **10**, 1130–1161.

[29] RUZAYQAT, H., BESKOS, A., CRISAN, D., JASRA, A., & KANTAS, N. (2024). Sequential Markov Chain Monte Carlo for Lagrangian Data Assimilation with Applications to Unknown Data Locations. *Quart. J. Roy. Met. Soc.*, **150**, 2418-2439.

[30] SRIVASTAVA, A., & KLASSEN, E. (2004). Bayesian and geometric subspace tracking. *Adv. Appl. Prob.*, **36**, 43-46.

[31] ZAPPA, E., HOLMES-CERFON, A. & GOODMAN, J. (2018). Monte Carlo on manifolds: sampling densities and integrating functions. *Comm. Pure Appl. Math.*, **71**, 2609-2647.

[32] ZEITOUNI, O. (2002). Approximate and limit results for nonlinear filters with small observation noise: the linear sensor and constant diffusion coefficient case. *IEEE Transactions on Automatic Control*, **33**(6), 595-599.

[33] ZHANG, C., TAGHVAEI, A., MEHTA, P. (2018). Feedback Particle Filter on Riemannian Manifolds and Matrix Lie Groups. *IEEE Trans. Aut. Contr.*, **63**, 2465–2480.